Eur. Phys. J. D **16**, 275–277 (2001)

THE EUROPEAN PHYSICAL JOURNAL D

EDP Sciences

Material characterization of a nanocrystal based photovoltaic device

M.M. Erwin[1], A.V. Kadavanich[1,2], J. McBride[1], T. Kippeny[1], S. Pennycook[2], and S.J. Rosenthal[1,a]

[1] Vanderbilt University, Dept. of Chemistry, Nashville, TN 37235, USA
[2] Oak Ridge Natonal Laboratory, Solid State Division, PO Box 2008, MS 6030, Oak Ridge, TN 37831-6030, USA

Received 30 November 2000

Abstract. Nanocomposites have shown promise as the active layer for photovoltaic energy conversion. One example is the CdSe nanocrystal\polymer composite demonstrated by Hyunh and Greenham [1,2]. In this paper we investigate the baseline properties of the materials used in such a device. We present surface chemical information for CdSe nanocrystals and chemical analysis for poly-(3-hexylthiophene) (P3HT) polymer.

PACS. 81.07.Pr Organic-inorganic hybrid nanostructures – 81.07.Bc Nanocrystalline materials – 82.35.Cd Conducting polymers – 68.37.Lp Transmission electron Microscopy (TEM) (including STEM, HRTEM, etc.) – 82.80.Yc Rutherford Back Scattering (RBS), and other methods of chemical analysis

1 Introduction

The conversion of sunlight directly into electricity using the photovoltaic properties of suitable materials is the most elegant form of energy conversion, second only to photosynthesis itself. The driving force for the development of more efficient photovoltaic devices is the realization that traditional fossil energy resources, coal, gas, and oil are not only limited, but they also contribute to unpredictable and possibly irreversible climate changes in the near future through the emission of carbon dioxide [3]. Conventional solid-state photovoltaics suffer two main drawbacks: first, they are expensive to manufacture and second, they rely on minority carrier lifetimes and hence are very sensitive to defects, limiting device efficiencies in the field. To overcome such limitations various groups have started to develop new photovoltaic device designs using a biomimetic approach that borrows design concepts from natural photosynthesis. These structures are based on wet-chemical synthesis of most components and rely on very efficient charge separations at three-dimensionally heterojunction interfaces. The former helps keep cost down, while the latter reduces carrier losses due to recombination. A well-known example of this approach is the electrochemical cell of Grätzel and its newer solid-state version, which uses a conducting organic material. Another example of photovoltaics that use the biomimetic approach is the Hybrid Organic\Inorganic nanocomposite. Two examples are the nanocrystal\polymer composites of Greenham *et al.* [1] and Huynh *et al.* [2]. In order to understand the photovoltaic properties and maximize the efficiency of such a nanocrystal based device, the underlying chemical and physical properties of each material and their interfaces need to be thoroughly investigated. We have used Scanning Transmission Electron Microscopy\Electron Energy Loss Spectroscopy (STEM\EELS) to investigate the interface between the nanocrystal and polymer. To investigate the polymer regioregular head-to-tail poly(3-hexyl thiophene) (HT P3HT), we have used Rutherford Backscattering Spectroscopy (RBS), Atomic Force Microscopy (AFM) and UV-vis spectroscopy.

2 Nanocrystal\polymer interface analysis using STEM\EELS

2.1 Sample preparation\experimental

CdSe nanocrystals were prepared by the method of Murray [6,7], as modified by Peng [8] for size-focusing. The TOPO surface ligands were exchanged with pyridine by heating in anhydrous pyridine for several hours. The nanocrystals were subsequently precipitated with hexanes and dissolved in chloroform. Poly (2-methoxy, 5-(2-ethyl-hexyloxy)-p-phenylenevinylene) (MEH-PPV) was prepared by the method of Wudl [9] and dissolved in chloroform. TEM samples were prepared by mixing the MEH-PPV and CdSe solutions and spin-coating onto single-crystal NaCl substrates (100 surfaces). EELS analysis was performed in a Vacuum Generators (VG) model HB501 STEM operating at 100 kV with an ultimate resolution of 2.2 Å. However, to optimize EELS data collection, the probe was run with low excitation of the condenser lens and the exact probe size was not measured. A parallel

[a] e-mail: sjr@femto.cas.vanderbilt.edu

EELS system using a CCD detector with near single-electron sensitivity was employed.

2.2 Results\conclusions

EELS spectra are collected in the range from 500 eV to 950 eV. The pre-edge background for each EELS spectrum is fit to a power law function and subtracted to obtain the Oxygen K-edge signal at 532 eV. Edge intensities are integrated in the range from 532 eV to 600 eV. To obtain the linescan shown in Figure 1, the probe was scanned immediately after acquiring the image. Another image was obtained after the scan to gauge specimen drift. Spectra were collected in seventeen 4 second increments while continuously scanning the probe along the line indicated in the figure. The total drift in the image for the entire linescan was about 10 Å, predominantly to the right, so that the positional uncertainty in each step is less than 1 Å. The edge intensities indicate the relative oxygen content as a function of position along the scan. The depletion of oxygen at the center of the nanocrystal is due to the exclusion of MEH-PPV. The slight increase at the edges of the nanocrystal is suggestive of a thin oxide shell viewed in projection segment. Based on the empirical formula for MEH-PPV ($C_{17}H_{24}O_2$) our acquisition parameters correspond to detecting less than 10 atoms of oxygen within a scan increment on the polymer substrate and less than 5 atoms at the center of the nanocrystal. The slight rise at the nanocrystal edge would be 1-2 atoms of oxygen at this scale. This is of course a rather crude estimate. We should also point out that scans at lower energy exhibit no indication of the nitrogen K-edge at 400 eV, which corroborates other observations [1,10] that the pyridine ligand is removed from the nanocrystals during processing into the thin film specimen. This will enhance the charge transfer at the nanocrystal\polymer interface as is desirable for photovoltaic applications [1,2,11,12].

3 Chemical analysis of the polymer matrix

3.1 Sample preparation

P3HT was purchased from Aldrich Chemical Co. as a loose solid. This polymer is prepared by the method of Rieke [13]. As-received samples were processed under a dry nitrogen environment in a dri-box. The powder was dissolved in dry chloroform (distilled from calcium hydride under ultra-high-purity argon) and stored in glass vials. Purified samples were obtained by successive extractions of the solid with methanol and hexanes for 24 hours each in a Soxhlet extractor in ambient air. After drying, the solid was transferred to the dri-box and treated in an analogous manner to the as-received sample. Analysis was run on two different batches of polymer, identified by their lot numbers (Aldrich Lot # 05006 MU PU and # 27723 JS AU). Polymer films were prepared on pieces of Silicon test wafers for Rutherford Backscattering Spectroscopy (RBS) analysis and on glass slides for optical and Atomic Force Microscopy (AFM) analysis.

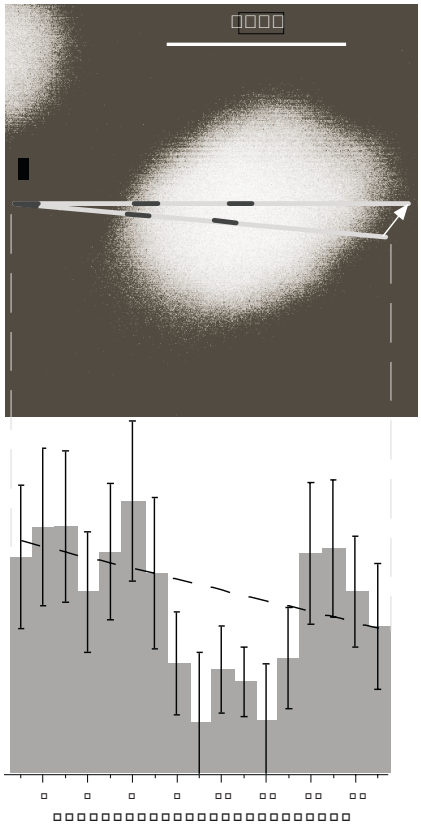

Fig. 1. Top: Dark field image of a single nanocrystal with the linescan indicated by the horizontal line. The marker in the center indicates the length of each scan step and thus the area integrated for each EELS measurement. Bottom: The oxygen concentration profile calculated from the EELS oxygen K-edge intensity at each scan step. The depletion at the center is attributed to the excluded volume of MEH-PPV.

3.2 Rutherford back scattering (RBS)

Analysis of the RBS data shows the presence of Zn and Br impurities in the as-received P3HT, but the amount of impurities were dramatically reduced in the purified P3HT. See Figure 2. The presence of impurities is of concern, as the work functions of both Zn and Br may permit them to act as carrier traps in a CdSe\P3HT device.

3.3 Atomic force microscopy (AFM)

Optical Absorption spectra were obtained on a Varian Cary 50 Bio UV-Visible spectrophotometer. Blank spectra were recorded and subtracted from each scan by the Cary software. AFM measurements were done on a Digital Instruments Nanoscope III AFM in Tapping Mode with Si cantilever tips. In the absence of impurities, the intensity of the main absorption peak is a good indicator of film thickness. In order to find the correlation between optical density and film thickness we therefore performed a series of optical and AFM studies for several thin films ranging in optical density from 0.01 to 2.01. After the optical spectrum was obtained for each thin film, to measure

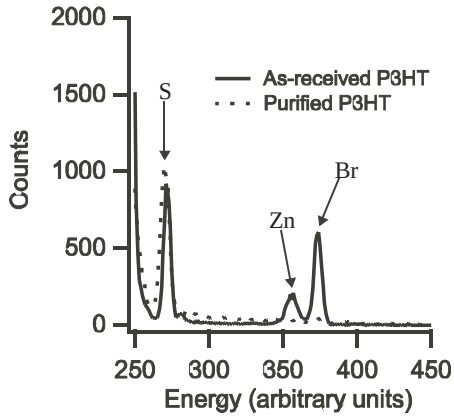

Fig. 2. RBS spectra for the as-received and purified P3HT. The spectra have been normalized to the height of the sulfur peak. Indicated are the impurity peaks. Based on the peak positions, these have been assigned to Zn and Br. The low energy region containing the Si and C signals are not shown.

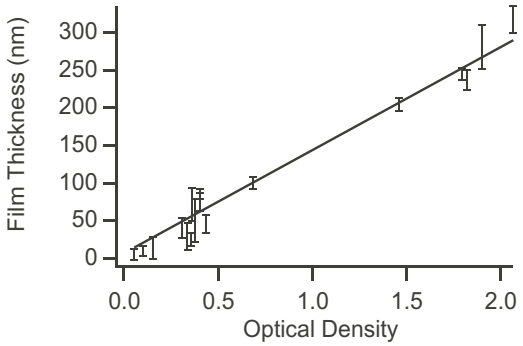

Fig. 3. Plot of P3HT film thickness as a function of absorbance at the maximum absorption wavelength. The error bars are calculated from the uncertainty in the height calibration and the RMS variance in the height measurements. The line indicates a weighted least squares fit to the data. Also shown is the 95% confidence interval for the fit.

thickness, the same polymer film was scored with a fresh razorblade and the resulting groove imaged in the AFM. The difference in the height between a small area of the groove and an adjacent area of the unperturbed film was taken as the film thickness. Heights were measured using the Nanoscope software's Roughness feature. This is demonstrated in Fig. 3, which represents the height of the main peak, in units of Optical Density ($O.D.$) as a function of the film thickness obtained by AFM. Also shown is a weighted least-squares fit to a line, represented by the function $t = (136.75 \pm 2.39)O.D. + (6.9089 \pm 1.95)$, where t is the polymer film thickness.

4 Conclusions

We have shown that in the CdSe\MEH-PPV composite the nanocrystal surface has a 0.5 to 1 oxide monolayer after processing. We have also seen that the CdSe pyridine surface ligands are removed during processing. In our chemical analysis of the polymer P3HT we found Zn and Br impurities in the commercially available polymer. We also report the first correlation between the intensity of absorbance peak and film thickness of P3HT thin films.

The National Renewable Energy Laboratory funded this work, subcontract No. AAD-9-18668-11 and by the National Science Foundation, under Career Award 9875875 and by the Department of Energy, Basic Energy Sciences, Materials Sciences Division contract No. DE-AC05-84OR21400. We would also like to thank Len Feldman for the use of the RBS instrument and Charles Lukehart for the use of the AFM instrument. AVK gratefully acknowledges the assistance of P.D. Nellist, B.E. Rafferty, G. Duscher and M.F. Chisholm in learning the operation of the STEMs.

References

1. N.C. Greenham, P. Xiaogang, A.P. Alivisatos, Phys. Rev. B: Cond. Matt. **54**, 17628 (1996).
2. W.U. Huynh, P. Xiaogang, A.P. Alivisatos, Adv. Mat. **11**, 923 (1999).
3. H.J. Möller, *Semiconductors for Solar Cells* (Artech House, Inc., 1993).
4. B. O'Regan, M. Grätzel, Nature **353**, 737 (1991).
5. Bach *et al.*, Nature **395**, 583 (1998).
6. C.B. Murray, D.J. Norris, M.G. Bawendi, J. Am. Chem. Soc. **115**, 8706 (1993).
7. J.E. Bowen Katari, V.L. Colvin, A.P. Alivisatos, J. Phys. Chem. **98**, 4109 (1994).
8. X.G. Peng, J. Wickham, A.P. Alivisatos, J. Am. Chem. Soc. **120**, 5343 (1998).
9. F. Wudl, G. Srdanov, in *United States Patent* (United States of America, 1993).
10. B.S. Kim, L. Avila, L.E. Brus, I.P. Herman, Appl. Phys. Lett. **76**, 3715 (2000).
11. D.S. Ginger, N.C. Greenham, Synth. Met. **101**, 425 (1999).
12. D.S. Ginger, N.C. Greenham, Phys. Rev. B: Cond. Matt. **59**, 10622 (1999).
13. X.W. Tian-An Chen, R.D. Rieke, J. Am. Chem. Soc. **117**, 233 (1995).